46th AIAA Aerospace Sciences Meeting and Exhibit
7 - 10 January 2008, Reno, Nevada

AIAA 2008-1076

Atmospheric Propagation Vs. Aero-Optics

John P. Siegenthaler[1], Eric J. Jumper[2], Stanislav Gordeyev[3]
University of Notre Dame, Notre Dame, IN, 46556

For decades the parameters of C_n^2, the Fried parameter (r_0), and the Greenwood frequency (f_G) have been used to characterize optically distorting flows and to guide the design of systems to correct the resulting distortions. However, their use has become so widespread that few stop to consider the origins and underlying assumptions of these terms. In recent years interest has grown in use of airborne optical systems, but it is questionable whether the aforementioned parameters can be applied to the conditions in the immediate vicinity of such systems in flight in a meaningful way. Despite this, there are ways of finding and expressing the relevant factors of such flows.

Nomenclature

AO	=	Adaptive Optics
A_p	=	Length or diameter of an optical aperture
C_A^2	=	Structure parameter associated with a structure function for variations in property *A*.
d	=	Diameter
d_a	=	Actuator spacing
$D_A(r)$	=	Structure function of variations in property *A* with respect to distance of separation *r*
DM	=	Deformable Mirror
$E(k)$	=	Kinetic energy spectrum, as a function of wavenumber
$E_A(k)$	=	Spectrum of intensity variations in property *A*, as a function of wavenumber
f	=	Frequency
f_G	=	Greenwood frequency
$g(x)$	=	Generic function of x
J_0, *J1*	=	Bessel functions of the first kind
K	=	General constant
k	=	Wavenumber
n	=	Index of refraction
OPD	=	Optical Path Difference
OPD_{rms}	=	Root mean square of OPD
OPL	=	Optical Path Length
P	=	Pressure
PSD	=	Power Spectral Density
r	=	Distance
r_0	=	Fried parameter
$_{\text{SubAp}}$	=	Length or diameter of a sub-aperture within an optical aperture
T	=	Temperature
t	=	Time
T/T	=	Tip-tilt
U_C	=	Convection velocity
V	=	Perpendicular velocity
v	=	Turbulent velocity
x	=	Position

[1] Graduate Research Assistant, Department of Aerospace and Mechanical Engineering, Hessert Laboratory, Student Member AIAA.
[2] Professor, Department of Aerospace and Mechanical Engineering, Hessert Laboratory, Fellow AIAA
[3] Professor, Department of Aerospace and Mechanical Engineering, Hessert Laboratory, Member AIAA

$\bar{x}$ = Time average of quantity x
$\varepsilon<\varepsilon>$ = Net dissipation in a flow
ε_A = Diffusion term related to property A.
θ = Phase
Λ = Length scale of a streamwise optical disturbance
σ_θ = Phase variance
λ = Wavelength of light

I. Introduction

MOST people concerned with turbulence-induced aberrations on the figure of a laser-beam's wavefront made to propagate through the turbulence fall into two camps; they are familiar with the physics and effects of propagation through either the atmosphere (atmospheric propagation) or high-speed turbulent flows in the vicinity of the beam-director's exit pupil (aero-optics). While the two propagation scenarios share the fact that the aberrations are imposed by index-of-refraction variations within the turbulence, little else about the characteristics of these two effects are the same. At the most-fundamental level, the causes of the index-of-refraction fluctuations are different. In the case of atmospheric propagation, the index-of-refraction variations are due to temperature fluctuations caused by very-large-scale (relative to the beam aperture) temperature gradients in a region of the atmosphere that itself is in shear and has turbulence scales that cascade from the largest scales down to sub-aperture scales. In this case, the temperature fluctuations are mixed, separated, and carried by the turbulence as a passive scalar. In the case of weakly-compressible flows aero-optic aberrations are caused by density fluctuations that form in and around the coherent structures in the turbulent flow.[1] Because of the direct connection between coherent-structure size and the amplitude of the density fluctuations, once the structures become small, they are no longer relevant to the optical problem (i.e., less than a 5% intensity reduction in the far field). It is these differences in cause and effect that make the characterization, prediction of effects and mitigation strategies so different.

At the heart of the field of atmospheric propagation is a single parameter, C_n^2. As will be discussed in detail below, C_n^2 depends on the turbulence, carrying the temperature passive scalar, being Kolmogorov. If the turbulence can be characterized as Kolmogorov this single parameter, C_n^2, describes not only the scale size of the aberrating index-of-refraction fluctuations, but also the magnitude of the aberration associated with them. Coupled with the velocity of the air normal to the laser beam, all of the relevant optical parameters of the aberrating turbulence can be deterministically derived, including the requirements for adaptive-optic mitigation systems. This is why the focus of requests for research in aero-optics in the late 1980's asked for determination of C_n^2 for aero-optic flows. Unfortunately, as will also be addressed in this paper, C_n^2 is irrelevant to the characterization of aero-optic turbulence since the range of scales over which aero-optic turbulence can be considered Kolmogorov places them below the scale sizes that are relevant to the optical problem.

Because both camps of researchers focus on dealing with index-of-refraction induced wavefront aberrations and mitigation approaches invariably make use of adaptive-optic schemes, it seems natural that researchers in both camps should collaborate; however, a general lack of understanding of the physical basis for each group's field of study directly impedes communication between camps. In fact, even many of the researchers in the two camps are so used to dealing with the constructs that have been developed for each field, they themselves are unfamiliar with the basis for their approaches and simply make use of parameters such as C_n^2, taking for granted that they need only the parameter and not the basis for its origin. It is this common misunderstanding of the basic concepts leading to parameters associated with atmospheric propagation and aero-optics that this paper attempts to address. In so doing, we first take up the theoretical basis for C_n^2 and associated parameters of the Fried parameter, r_0, and the Greenwood frequency, f_G, that are associated with atmospheric propagation. This discussion is followed by a general description of aero-optic aberrations caused by separated shear layers. This discussion includes an approach to inferring the relevant scale sizes and aberration amplitudes associated with shear-layer-induced aero-optic effects.

II. Atmospheric Propagation

As noted previously, the standard models of the atmosphere used to express and predict the optical effect upon light propagating through that atmosphere are based upon a set of simplifying assumptions.

A. Kolmogorov Turbulence

The Kolmogorov model of turbulence is a statistical, incompressible model, based largely on the idea of energy being transferred between various length scales in the flow. At the largest scales are persistent eddies that act as the energy supply for the turbulent flow. At the smallest scales, viscous forces become dominant, and the kinetic energy

in the flow is dissipated, becoming heat. Between those two extremes is an inertial range of scales, in energy is neither added nor dissipated, but may be transferred from one scale to another. Figure 1 shows a sketch of the expected form of this spectrum. The peak in this curve corresponds to the length scale of the large eddies, while the downturn at larger wavenumbers reflects the viscous dissipation occurring at smaller length scales.

In characterizing this behavior, it is assumed that the flow has reached an equilibrium state, in which the energy being transferred to a given length scale in the inertial range equals the energy being transferred from that length scale to other scales. As part of this equilibrium state it is assumed that energy has also spread evenly to all locations in the flow and all axes of orientation, so that the flow is homogenous and isotropic.

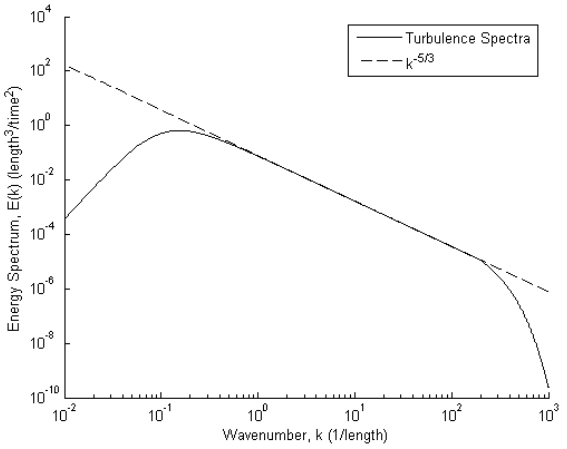

Figure 1. A sketch of a turbulent energy spectrum.

Kolmogorov[2] proposed that in fully developed turbulence of this sort, the properties in the inertial range were only dependent upon the flux of energy through those scales. If the assumed equilibrium is to be maintained, then energy must be transferred from the large scales to the small scales at a rate such that the total energy flux through a length scale of the inertial range must equal the net dissipation (<ε>) occurring at the smaller scales. From this comes the expression for the kinetic energy spectral density presented in Eq. 1.

$$E(k) = K\langle\varepsilon\rangle^{2/3}k^{-5/3} \tag{1}$$

The exponents in Eq. 1 are the result of dimensional analysis. $E(k)$ has units of velocity-squared per wavenumber, which can be written as length-cubed over time-squared. K is a numerical constant, the dissipation term (<ε>) has units of length-squared over time-cubed, and the wavenumber (k) has units of length to the -1 power. This -5/3 power law to describe the inertial range has been verified in numerous experiments.[3]

B. Structure Functions and C_n^2

Related to this concept of a kinetic energy spectrum is the expression of a velocity structure function, defined as the average of the square of the difference in turbulent velocity observed at two points separated by some distance r.

$$D_v(r) = \overline{\left(v(0) - v(r)\right)^2} \tag{2}$$

As the flow is assumed to be homogenous and isotropic, neither the location of the first point, the orientation of the path between the points, nor the direction of the velocity component under consideration should have an effect on this structure function. A sketch of the expected form of this structure function over all scales is shown in Fig. 2. It should be kept in mind when relating this to the energy spectrum of Fig. 1 that the horizontal axis in this figure represents the separation distance r, with units of length, rather than wavenumbers with units of 1/length.

At the small scales, the structure function goes rapidly to zero with decreasing r as dissipation and diffusion even out variations at those scales. At the larger scales, the structure function levels of to a constant value, as the flow observed at the two points becomes completely decoupled with large distances of separation. In the range of scales between, just as

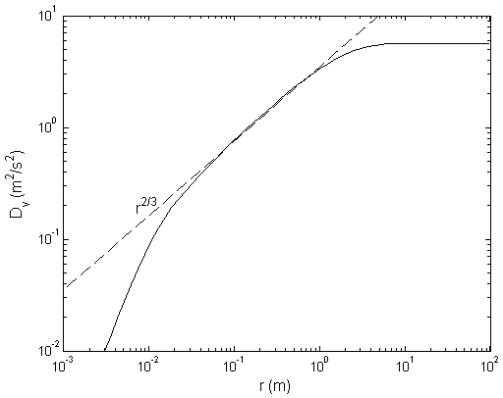

Figure 2. A structure function for velocity variations in turbulent flow.

the energy spectrum has an inertial region characterized by $k^{-5/3}$, the structure function has a range in which it can be described by the expression:

$$D_v(r) \cong C_v^{\,2} r^{2/3}. \tag{3}$$

In the expression of Eq. (3), C_v^2 is a constant to fit this approximation to a particular case, and to match units. As more energetic flows will have greater fluctuations in observed turbulent velocity, this constant will rise and fall with the turbulent energy of the flow and can be used as an indicator of the severity of the turbulence.

Obukhov[4], examined the temperature field to be found in turbulence of this type, treating temperature as a passive scalar which is carried with the flow and may diffuse into the flow, but has negligible effect upon the behavior of the flow. Performing a similar analysis to that of Kolmogorov, he found that the variations in concentration or intensity of such passive scalars could be expressed in terms of an energy spectrum, and while the expression for this spectrum included an additional diffusion term (ε_T) the dimensional analysis produced the same -5/3 power law with respect to wavenumber.

$$E_T(k) = K\langle\varepsilon\rangle^{-1/3}\varepsilon_T k^{-5/3} \tag{4}$$

Likewise, this temperature energy spectrum has an associated structure function, $D_T(r)$ which can be approximated by $D_T(r) \cong C_T^2 r^{2/3}$ over the appropriate range.

Tatarski[5] then built upon the work of Kolmogorov and Obukhov, relating this to the effect upon waves propagating through the atmosphere. Variations in temperature and pressure of a gas or collection of gasses will produce variations in density. By the Gladstone-Dale relationship[6], these variations in density in turn produce variations in the index of refraction (n). In air, for wavelengths in or near the visible range, this relationship can be approximated as[7]

$$dn = 7.77 \cdot 10^{-7} \frac{P}{T}\left(\frac{dP}{P} - \frac{dT}{T}\right) \tag{5}$$

As noted, Kolmogorov turbulence is assumed to be an incompressible flow. In the free atmosphere, pressure gradients severe enough to produce significant density variation on the length scale of most optical path diameters tend to disperse at sonic speeds and the small pressure fluctuations that are coupled to velocity variations in atmospheric turbulence tend to have a low order optical impact compared to the effect of temperature fluctuations[8]. Under these conditions with these applicable approximations, one would then expect a structure function with respect to the index of refraction, $D_n(r) \cong C_n^2 r^{2/3}$, such that

$$C_n^2 = \left(\frac{7.77}{10^7}\frac{P}{T^2}\right)^2 C_T^2 \cdot \tag{6}$$

Thus, C_n^2, which is often used as the indicator of the strength of optical turbulence, has its origin as the parameter in an $r^{2/3}$ fit to the index of refraction structure function, based on a structure function of temperature variations, based on Kolmogorov turbulence and the underlying assumptions thereof. It should also be kept in mind that the fit of which C_n^2 is a parameter only applies over the inertial range of the turbulence. In most optical applications dealing with atmospheric flows, it is reasonable to assume that the large scale is so large as to have little effect on an optical path, and the small scale contains relatively little energy.

C. The Fried Parameter

As noted in the introduction, variations in n produce variations in a wavefront of light as it propagates through those variations. As light travels slower in areas with a higher index, the same absolute path length becomes effectively longer or shorter from an optical standpoint in regions of greater or lesser n. The Optical Path Length (OPL) can then be found by integrating through the values of n encountered along the path.

$$OPL = \int_{s_1}^{s_2} n(s)ds \tag{7}$$

Often of more interest at the receiving point of the light is the Optical Path Difference (*OPD*), which is the *OPL* with the mean removed, leaving only the relative differences in that path length. These path length differences can then be scaled by the wavelength of the light (λ) to indicate differences in phase (θ) over the receiving plane.

$$\theta(x, y) = \theta_0 - \frac{2\pi}{\lambda} OPD(x, y) \tag{8}$$

Differences in phase produce differences in amplitude and intensity as a wave propagates. This focus on *OPD* and phase differences is one reason why the large scale of Kolmogorov turbulence can often be ignored, as variations induced on a scale larger than a desired field of view or the diameter of a directed beam become irrelevant to a particular optical application. One may define structure functions of phase variations (D_θ) and log-scale amplitude variations ($D_{\ln(A)}$) seen at a receiving plane, much as structure functions are defined for properties in the flow. If the flow is such that its optical effects over the relevant length scales can be characterized by C_n^2, then a combined structure function in variations seen at the receiving plane can be found as

$$D_\theta(r) + D_{\ln(A)}(r) = 2.91\left(\frac{2\pi}{\lambda}\right)^2 r^{5/3} \int_{s_1}^{s_2} C_n^2(s)ds \,. \tag{9}$$

This structure function goes according to $r^{5/3}$ instead of $r^{2/3}$, because these variations are a result of integrating through all of the index variations described by an $r^{2/3}$ structure function.

Fried[9] assumed that if one was attempting to recover information from light received through an aperture, then there would be some signal modulated onto a carrier wave, such that the amplitude of the carrier would be much greater than the amplitude of the signal. This modulation might be one of amplitude, phase, or frequency. Based on this assumption, a circular aperture of diameter *d*, and a combined structure function of the form in Eq. (9), a normalized signal to noise ratio can be written in terms of *d*, normalized by some length scale r_0:

$$\psi\left(\frac{d}{r_0}\right) = \frac{32}{r_0^2 \pi} \int_0^d \frac{1}{2}\left(\cos^{-1}\frac{r}{d} - \frac{r}{d}\left(1 - \left(\frac{r}{d}\right)^2\right)^{1/2}\right) e^{-\frac{6.88}{2}\left(\frac{r}{r_0}\right)^{5/3}} r dr \,. \tag{10}$$

This function, shown in Fig 3, is asymptotic to a constant value for large diameters, and proportional to the square of the diameter for small apertures. The reasons for this can be visualized by starting with an infinitesimal aperture. As the aperture is enlarged the area of the aperture increases with the square of the diameter, and proportionally more light is captured, providing more signal strength to work with and improving the signal to noise ratio. However, a larger aperture also captures larger propagation-induced variations at the plane of the aperture, per Eq. (9). Thus a point of diminishing returns is reached.

Setting r_0 such that Eq. (9) equals $6.88(r/r_0)^{5/3}$ normalizes the curve of Eq. (10) to a value of 1 over the larger apertures and places the intersection of the two asymptotes at the point where $d/r_0 = 1$. The behavior of this signal to noise function also indicates that having an aperture larger than this value of r_0 will not significantly improve the signal to noise ratio of a signal or resolution of an image. Taking the right-hand portion of Eq. (9), setting it equal to $6.88(r/r_0)^{5/3}$, and rearranging, r_0 can be found to be:

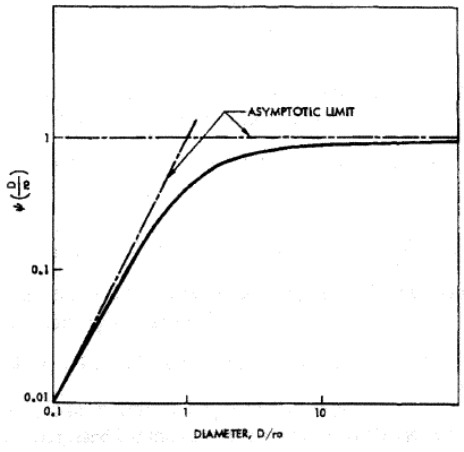

Figure 3. Fried's normalized signal-to-noise ratio.[9]

$$r_0 = \left(0.423 \frac{4\pi^2}{\lambda^2} \int_{s_1}^{s_2} C_n^2(s)\, ds \right)^{-3/5}. \tag{11}$$

As r_0 also represents a limit in improving the resolution of an image, it is often identified as the size of the largest aperture that can be considered diffraction limited. However, this is an inherently imprecise definition, as any variation from a planar or spherical wave over the aperture will result in a deviation from the diffraction-limited case, even if that deviation is vanishingly small.

It so happens that the value of r_0 arrived at as above is such that the mean-squared average of phase variations observed within a circular aperture of diameter r_0 is about 1.04 radians-squared. Thus, a more quantitative physical interpretation often given for r_0 is that it is the size of an aperture over which the root-mean-square phase variance is approximately 1 radian. This commonly given definition of r_0 is an incidental byproduct that is a few steps removed from the basis of its definition.

In the design of systems for optical compensation and correction, r_0 serves as a guideline for how many actuators are needed within an interval for effective correction. If a continuous reflective sheet is used for correction, and the actuators driving this sheet are separated by some distance d_a, then the expected phase variance remaining after correction (σ_r), in radians squared, would be[10]

$$\sigma_r^2 = 0.28 \left(\frac{d_a}{r_0} \right)^{5/3} rad^2. \tag{12}$$

D. The Greenwood Frequency

Turbulence is rarely stationary. As winds carry turbulence through an optical path, or an optical path is slewed through the atmosphere to track a target in relative motion, the distortions induced by the atmosphere will appear to move across the aperture. This motion will relate the aforementioned length scales to temporal frequencies.

Fried and Greenwood coauthored a paper[11] examining the power spectra of phase variations seen at an aperture, with regards to the bandwidth required from actuators driving a segmented mirror to correct these aberrations. They found power spectra associated with a deformable mirror for correcting piston alone, power spectra for tilt correction, and differences in these spectra for segments on the edges of the segments surrounded by and influenced by other segments of the mirror. While this level of detail in their analysis is laudable, it is also a bit much for providing guidance in engineering applications. With this in mind, Greenwood[12] simplified their work by first looking at the case of piston-only correction, and then taking the limit as the segment size shrunk to zero. From this, the power spectral density (PSD) for phase variations at an infinitesimal point in the aperture is found to be:

$$PSD_\theta(f) = 0.0326 \left(\frac{2\pi}{\lambda} \right) f^{-8/3} \int_{s_1}^{s_2} C_n^2(s) \left| V(s) \right|^{5/3} ds, \tag{13}$$

for an optical path from s_1 to s_2. This expression allows for possible variations along the path in and the mean velocity perpendicular to the path of propagation. (V)

Any form of optical correction applied is likely to have some frequency response, which can be expressed as a complex function, $H(f,f_c)$, with f_c indicating a characteristic frequency of the system. This correction will effectively filter out part of the aberrations. The power spectral function of the residual, uncorrected phase error (PSD_r) will then be

$$PSD_r(f) = \left| 1 - H(f, f_c) \right|^2 PSD_\theta(f). \tag{14}$$

The rms phase variance (σ_θ) and residual phase variance after correction (σ_r) seen at the point in question corresponds to the square root of the integral of these power spectra over all frequencies.

$$\sigma_r^2 = \int_0^\infty PSD_r(f)\, df = \int_0^\infty \left| 1 - H(f, f_c) \right|^2 PSD_\theta(f)\, df. \tag{15}$$

If the frequency response is assumed to have the form of a simple RC-filter,

$$H(f, f_c) = (1 + i \cdot f / f_c)^{-1}, \tag{16}$$

then for a desired value of σ_r one should design a system with a characteristic frequency such that

$$f_c = \left[0.102 \left(\frac{2\pi}{\lambda \sigma_r} \right)^2 \int_{s_1}^{s_2} C_n^2(s) |V(s)|^{5/3} ds \right]^{3/5}. \tag{17}$$

As noted, the Fried parameter is associated with phase variances over an aperture with an rms value of 1 radian. This value of 1 radian has also become associated with a manageable or acceptable level of phase variance, so it has become common practice to set σ_r in Eq. (17) to a value of 1 radian and to call the resulting value for f_c the Greenwood frequency. This frequency is commonly used as a guideline for the bandwidth required of a corrective system intended to deal with optical turbulence.

III. Aero-Optics

As was previously noted, the atmospheric models and related analysis and predictions of optical turbulence are based on a number of simplifying assumptions. The atmosphere is expected to be in equilibrium, to be interacting only with itself, and to be adequately described by incompressible forms of the Navier-Stokes equations. The standard expressions for optical turbulence make further assumptions that all length scales of interest are associated with the inertial range of Kolmogorov turbulence and that variations in density and *n* are due solely to variations in temperature.

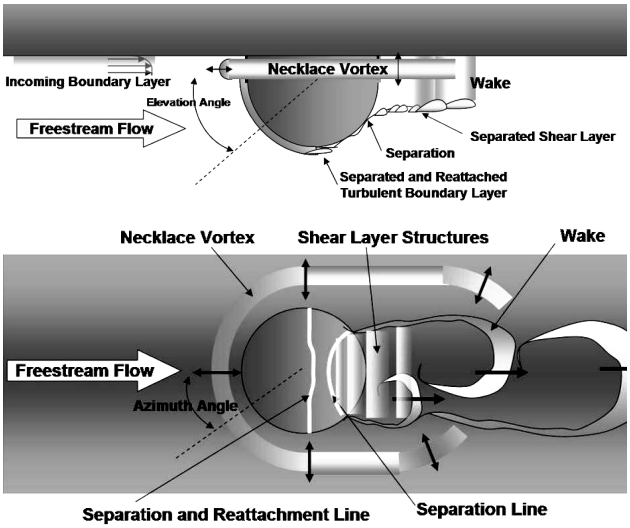

Figure 4. Examples of aero-optic flows.

Aero-optics deals with the flow around physical objects, particularly the mounting for an optical system and what ever that system is mounted on. Figure 4 shows a sketch of various flows that might be seen around a hemispherical turret mounted on a surface. There is an incoming boundary layer along the surface upstream of the turret, a necklace vortex around the base of the turret, regions of separation and reattachment, a shear layer associated with the separation region, and a wake with von Karman vortex shedding. One thing that is immediately obvious from this figure is that the flow may have very different characteristics depending on the location and orientation within the flow, which means the assumptions of isotropy and homogeneity do not apply.

If the freestream velocity indicated in Fig. 4 is low enough that these flows can be considered incompressible, which is likely to be the case for a ground-based system, then the optical effect of these flows is likely to be negligible. However, recent decades have seen increasing interest in the use of airborne optical systems, with the associated velocities required to keep many such systems in the air.

A. Compressible Shear Layers

Experimental studies of transonic flows over configurations such as the one shown in Fig. 4 have demonstrated that the resulting flow structures are indeed a source of optical aberrations.[13] Studies of transonic shear layers in particular have shown that the rolling vortices making up such flows contain significant wells of low pressure[14] not predicted by incompressible theories, and that these low pressure regions can produce significant optical distortions not predicted by models based solely on temperature differences.[15] Figure 5. shows a PSD for the deflection of a narrow beam passed through a shear layer comprised of a Mach 0.8 flow and a Mach 0.1 flow, at a point 13.4 cm downstream from the origin of the shear layer. The peak in this spectrum occurs at a frequency corresponding to that

of the "rollers" being carried by at the convective velocity. This frequency can be related to a length scale, Λ, by the convective velocity (U_C) and the relationship

$$f = U_C / \Lambda . \tag{18}$$

Figure 6. shows a plot of these length scales based on the peak frequencies of PSDs generated from data taken at multiple points in the Mach 0.8 shear layer. Once the shear layer has fully developed, this vortex spacing grows linearly with position. This is to be expected, as the thickness of a shear layers grows linearly as it progresses downstream, and it may be anticipated that streamwise dimensions would grow in the same manner. What is significant about these length scales is that they are on the order of the distance downstream, having a ratio of $\Lambda/x \cong 0.42$.

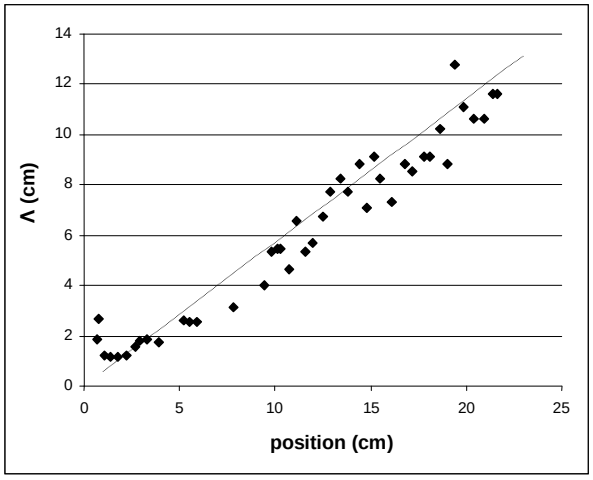

Figure 6. Optical disturbance length with shear layer position.

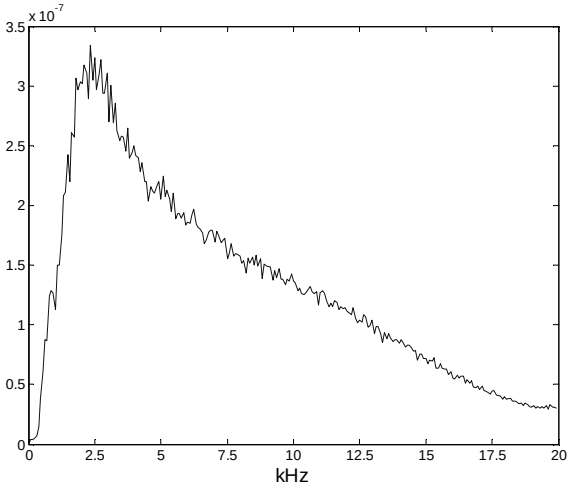

Figure 5. Beam Jitter PSD from a compressible shear layer.

Shear layers are of particular interest in aero-optics as they may form over cavities or in any instance of separated flow. Because of this, they are among the flows most likely to occupy a position directly in a desired optical path. Referring back to Fig. 4, if a beam director or receiving aperture were located on the turret, then any look angle directed downstream would be likely to have part of the separation region and associated shear layer covering a portion of the optical aperture in the turret. If the optical system were recessed into the surface instead of projecting out from the surface, then the resulting cavity flow would also have a shear layer in the optical path.

From Figs. 5 and 6, it can be seen that the length scales containing the most energy and highest degree of variations of n in such shear layers will not be significantly larger than the diameter of the optical path in question, but may in fact be on the order of the path diameter or somewhat smaller. Because of this, the sources of significant optical distortion in these flows can not be characterized by the -5/3 power law of Kolmogorov turbulence or the 2/3 law of an associated structure function. Therefore there is no value of C_n^2 such that the expression $r^{2/3}C_n^2$ will approximate the optical characteristics of the flow, and Eqs. 9, 11, 13, 17 and any other expression dependent upon C_n^2 and this approximation can not be relied upon. Having a dominant or peak frequency in the observed jitter signals has also been observed in flow over a turret[13] of the sort in Fig. 4. despite the fact that such flow may correspond only partially to a canonical shear layer. It has also been observed in compressible boundary layers.[16]

While aero-optic flows do not follow the aforementioned rules of scale for atmospheric flows, they do tend to have a characteristic length scale and associated frequency, as shown for shear layers in Figs. 5 and 6. This is because these flows are not in the equilibrium state that is assumed for Kolmogorov turbulence, in which energy would have spread to all locations, length scales, and axes of orientation. Instead the significant contributors to optical distortion in aero-optic flows tend to be found in a band of length scales and frequencies, produced by the interaction of the flow with some physical object and short-term development of the flow thereafter. Over time, the energy introduced in this manner is likely to be dispersed and transferred until it reaches the Kolmogorov state, but by then it will most likely have passed far downstream and out of the optical path. Since the primary sources of optical distortion are associated with a relatively narrow set of frequencies, then it may be possible to examine the effects by approximating the distortions with a single frequency and length scale.

This is not to say that Kolmogorov turbulence may not be observed in these flows. In fact, it will most likely be present in the incoming air, as well as being the eventual end state for energy introduced into the flow through interaction with a turret or other physical structure. A self-similar range of sorts can be observed at higher frequencies in much of the data gathered in studying aero-optic flows.[13,16,17] However, by definition, the energy associated with those frequencies is less than that for the peak frequency and these Kolmogorov-style effects are likely to be of secondary importance relative to the effect of compressible coherent structures, provided those structures are on the order of, or smaller than the diameter of the optical path through the flow.

The nature of the spectrum and length scales associated with these flows and the role of pressure variations in producing optical distortions is significant as it separates the field of aero-optics from other studies of non-Kolmogorov turbulence. Other studies[18,19,20] have commonly dealt with types of atmospheric turbulence, in which the flow may still be self-similar, characterized by a power law even if it is not the power-law predicted my Kolmogorov. Even in cases in which this does not apply, the mechanism producing optical effects has still been assumed to be temperature-based, rather than due to compressible pressure effects.

B. Tip-Tilt Correction

The original goal of these studies was to provide optical correction. A partial schematic of the system to be used in providing this correction is shown in Fig. 7. An important aspect of this system is that the correction is provided in two stages. The first stage is a flat mirror mounted on actuators and used to center the beam onto a quad-cell sensor. This form of beam steering to keep the system centered on a target will hereafter be referred to as tip-tilt or T/T correction. The second stage of correction uses a deformable mirror (DM) to remove the phase variances remaining on the wavefront after it has been redirected by the T/T mirror. Two-stage correction of this type, with a beam-director or tracking system and a system for higher-order corrections as separate subsystems, is a fairly common arrangement in applications for adaptive optics (AO).

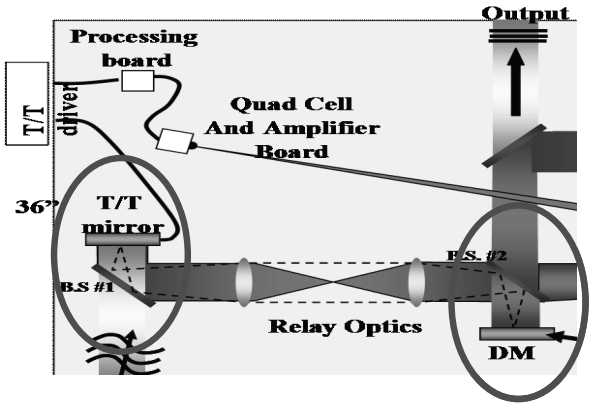

Figure 7. Two-stage optical correction in the Notre Dame AO system.

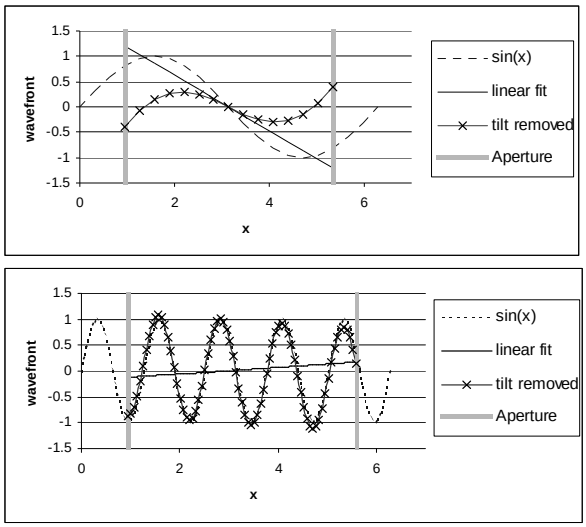

Figure 8. T/T correction for different length scales.

Figure 8 shows two examples of T/T correction for a wavefront distorted into the form of a sine wave, modeling an aero-optic distortion with a single characteristic frequency and length scale. It should be noted that tilt, in this case is defined as a linear fit to the wavefront over the indicated aperture. This definition of tilt, known as Zernike tilt or Z-tilt, differs from gradient tilt or G-tilt,[21] which would be an average of the slopes and gradients observed within the aperture. Preliminary studies at Notre Dame indicate that Z-tilt more closely corresponds to the tilt measurement provided by a quad cell, as is used in the in-house AO system at Notre Dame, while a true centroiding system tends to indicate G-tilt.[22]

The first example in Fig. 8 shows a simulated wavefront with a sine-shaped distortion of a length scale larger than the aperture. Over this aperture, containing only part of a single cycle of the disturbance, significant tilt is observed and removing this tilt greatly reduces the magnitude of the distortions within the aperture. The simulated wavefront in the second example of Fig. 8 has an aberration of the same amplitude, but with a higher frequency and shorter length scale, so that multiple cycles of the disturbance can be observed within the aperture. The linear fit representing Z-tilt across the aperture indicates very little tilt and removing this tilt has negligible effect upon the amplitude of the disturbance.

C. The Aperture Filter

As was discussed in section II.D, the Greenwood frequency was arrived at by envisioning a possible corrective system as a filter with a transfer function that removed optical distortions to greater or lesser effect at different frequencies. This can be done with T/T correction. For this study, the gain on this filter (G) is defined as the time-averaged rms OPD (OPD_{rms}) remaining within an aperture after T/T correction, divided by the OPD_{rms} without correction, which also corresponds to the OPD_{rms} observed over an infinite aperture with correction.

$$G(A_p) = \frac{\left(\overline{OPD_{rms}}(A_p)\right)^2}{\left(\overline{OPD_{rms}}(A_p = \infty)\right)^2} \tag{19}$$

For a wavefront of the form $g(x,t)$, OPD_{rms}, as a function of time over an aperture with T/T removal, will be:

$$OPD_{rms}\left(A_p, t\right) = \sqrt{\int_0^{A_p} \left\{ g(x,t) - \left[A(t) + xB(t)\right] \right\}^2 dx} \tag{20}$$

where A and B in Eq. 20 are the coefficients of a linear fit to the overall tilt and piston present in $g(x,t)$. It just so happens that finding values for A and B to minimize the function inside the square root in Eq. 20 is the basis for performing such a linear fit, which explains why T/T removal tends to reduce the magnitude of aberrations. These equations represent a one-dimensional aperture, of the sort shown in the examples of Fig. 8. This analysis can also be performed over a two-dimensional circular aperture with an additional coefficient and an additional integration for the second dimension.

$$OPD_{rms}\left(A_p, t\right) = \sqrt{\int_{-\sqrt{(A_p/2)^2 - x^2}}^{\sqrt{(A_p/2)^2 - x^2}} \int_{-A_p/2}^{A_p/2} \left\{ g(x,t) - \left[A(t) + xB(t) + yC(t)\right] \right\}^2 dxdy} \tag{21}$$

By setting the modeled disturbance, $g(x,t)$ to a sine wave of period Λ and varying this period, it can be found that the effective gain for a T/T corrective system across a one-dimensional aperture can be expressed as

$$G\left(\frac{A_p}{\Lambda}\right) = \frac{-3 - \pi^2\left(\frac{A_p}{\Lambda}\right)^2 + \pi^4\left(\frac{A_p}{\Lambda}\right)^4 + \left(3 - 2\pi^2\left(\frac{A_p}{\Lambda}\right)^2\right)\cos^2\left(\pi\frac{A_p}{\Lambda}\right) + 6\pi\frac{A_p}{\Lambda}\sin\left(\pi\frac{A_p}{\Lambda}\right)\cos\left(\pi\frac{A_p}{\Lambda}\right)}{\pi^4\left(\frac{A_p}{\Lambda}\right)^4}, \tag{21}$$

while T/T correction over a circular aperture has a gain of

$$G\left(\frac{A_p}{\Lambda}\right) = \frac{-\left(4\pi\frac{A_p}{\Lambda}J_0\left(\pi\frac{A_p}{\Lambda}\right)\right)^2 + \left(\pi\frac{A_p}{\Lambda}\right)^4 - \left(8J_1\left(\pi\frac{A_p}{\Lambda}\right)\right)^2 + 64\pi\frac{A_p}{\Lambda}J_0\left(\pi\frac{A_p}{\Lambda}\right)J_1\left(\pi\frac{A_p}{\Lambda}\right) - \left(2\pi\frac{A_p}{\Lambda}J_1\left(\pi\frac{A_p}{\Lambda}\right)\right)^2}{\left(\pi\frac{A_p}{\Lambda}\right)^4} \tag{22}$$

J_0 and J_1 indicate Bessel functions of the first kind. Of course, this analysis assumes that there is no error in measuring the wavefront or delay in implementing the correction. Equations 21 and 22 are plotted in Fig. 9. The non-denominational "frequency" of A_p/Λ can be linked to a real frequency by scaling by the aperture size in a particular case and through applying Eq. 16. The one-dimensional version has a 50% (3-dB) cutoff around $A_p/\Lambda = 0.85$, while this occurs near $A_p/\Lambda = 0.93$ for the two-dimensional circular aperture.

While this analysis is based upon a very simplified model of the optical distortions as a sine wave, it should be possible to build up any disturbance out of a Taylor series of sine and cosine functions. Additionally, these filter functions have been found to accurately describe the effect of T/T correction within an aperture upon the somewhat wider range of frequencies found in a shear layer as shown in the PSD of Fig. 5 and even in tracking tests through optical distortions based on Kolmogorov models.[23]

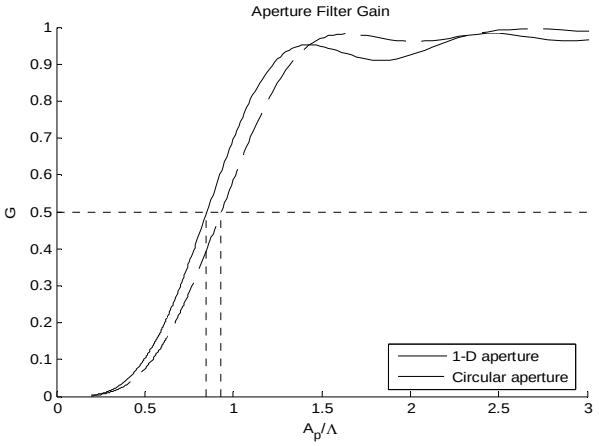

Figure 9. Effective gain for T/T correction over an aperture.

D. Higher-Order Correction

While this analysis provides guidelines for the effectiveness and frequency requirements of a T/T system to be applied in a given set of conditions, it does not fully provide substitutes for the commonly used indicators of atmospheric propagation. The values of r_0 and f_G are often applied in the design of higher-order corrective systems, not just T/T correction.

To explore these effects, the simple sine-wave optical disturbance model is once again applied. However, instead of a single linear fit across the entire aperture, the aperture is divided into a number of sub-apertures. A linear fit is applied to the simulated wavefront across each sub-aperture, with the condition that the endpoints of these linear functions must match at the boundaries between sub-apertures. It is, in effect, a first-order spline fit to the wavefront over these regions, intended to represent a correction system in the form of a segmented mirror, as represented by the drawing in Fig. 10.

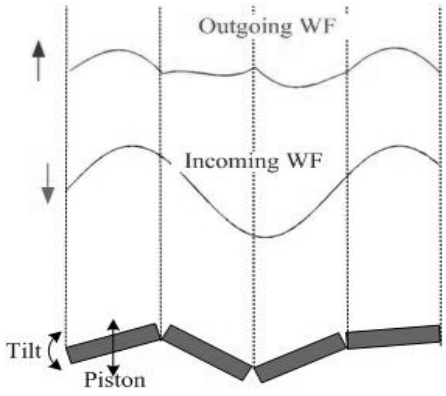

Figure 10. Segmented mirror / first-order spline correction.

Results of simulated corrections of this sort are shown in Fig. 11. As one might expect, applying correction over an increasing number

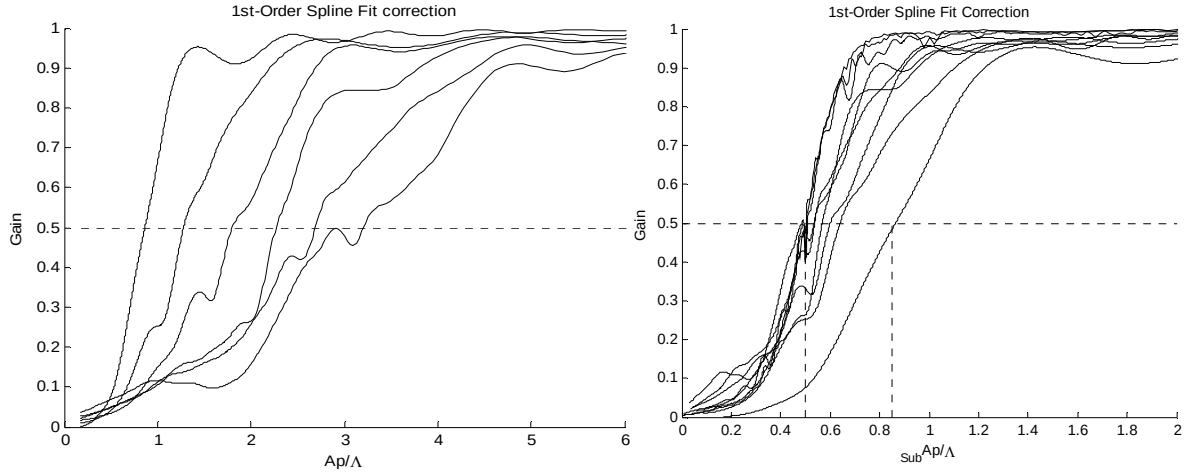

Figure 11. Results of simulated first-order spline correction (a) scaled to full aperture dimensions (b) scaled to sub-aperture dimensions.

of smaller sub-apertures within a fixed aperture allows a corrective system to deal with optical distortions associated with smaller length scales and higher frequencies. This is shown by the gain curve moving to the right with increasing number of sub-apertures in Fig. 11a. However, the endpoint condition imposed at the boundaries between sub-apertures causes the shape of this curve to change as more sub-apertures are added.

Figure 11b scales the results seen in Fig 11a by the dimensions of the sub-aperture ($_{sub}A_p$) rather than the full aperture, and includes results for 20, 50, and 100 sub-apertures. From this, it would appear that a corrective system of this sort converges on a smooth curve. An analytic expression for this curve has not yet been found, but it appears to have a 50% cut-off at a point of $_{sub}A_p/\Lambda \cong 0.5$. This would seem to indicate that a minimum of two sub-apertures per length scale of an expected disturbance is required for effective optical correction. Again, these non-dimensional ratios can be tied to a frequency and a bandwidth requirement for actuators driving the corrective system through Eq. 18.

IV. Conclusion

Models of atmospheric turbulence and the associated optical distortions are based on assumptions and conditions that are unlikely to be applicable in the case of aero-optic flows. Because of this, a number of standard indicators for aspects of the flow and guides to engineering compensation for the optical effects of the flow may be ill-defined or applied in misleading ways. However, the nature of those flows is likely to suggest a characteristic length scale and frequency, though this must be judged on a case by case basis, and may change with look angle through the flow. While the necessary guidelines for actuator spacing and bandwidth for designing an optical system for correction and compensation can be found for aero-optic flows, there is currently no single number or parameter that will sum up all aspects of the flow as C_n^2 does for atmospheric propagation. It might be possible to find an equivalent for C_n^2 based on Strehl ratios or phase-variance produced by a flow, but this would be misleading as these flows do not have the properties that define and in turn are defined by C_n^2.

Acknowledgments

These efforts were sponsored by the Air Force Office of Scientific Research, Air Force Material Command, USAF, under Grant Number FA9550-06-1-0160. The U.S. government is authorized to reproduce and distribute reprints for governmental purposes notwithstanding any copyright notation thereon.

References

[1]Fitzgerald, E. J. and Jumper E. J., "The optical distortion mechanism in a nearly incompressible free shear layer," *Journal of Fluid Mechanics*, Vol. 512, 2004, pp. 153-189.

[2]Kolmogorov, A. N., "On Degeneration of Turbulence in Incompressible Viscous Fluid." *C.R. Akad. Sci. SS*R (Dokl.) Vol 31, No. 6, 1941, pp. 538-541.

[3]Streenivasan, K. R., "On the Universality of the Kolmogorov Constant", *Phys. Fluids*, Vol. 7, No. 11, pp. 2778-2784.

[4]Obukhov, A. M., "Temperature Field Structure In a Turbulent Flow", Izv. AN SSSR (Geogr. and Geophys. series), 13, 1949, pp. 58–69.

[5]Tatarski, V. I., *Wave Propagation in a Turbulent Medium*, McGraw-Hill, New York, 1961.

[6]de Jonckheere, R., Chou, D. C., Miller, D. J., Jumper, E. J., "An Engineering Approach to Optical Phase Distortion Through Turbulent Thermal Boundary Layers", AIAA 20th Fluid Dynamics, Plasma Dynamics, and Lasers Conference, Buffalo, New York, June, 1989.

[7]Jumper, G. Y. and Beland, R. R., "Progress in the Understanding and Modeling of Atmospheric Optical Turbulence", 31st AIAA Plasmadynamics and Lasers Conference, Denver, Colorado, June 2000.

[13]-Gordeyev, S., Post, M., McLaughlin, T., Ceniceros, J., Jumper, E. J., "Aero-Optical Environment Around a Conformal-Window Turret," *AIAA Journal*, Vol. 45, No. 7, July 2007, pp. 1514-1524

[8]Friehe, C. A. et. al., "Effects of Temperature and Humidity Fluctuations on the Optical Refractive Index in the Marine Boundary Layer", *J. of the Optical Soc. of America*, Vol. 65, No. 12, Dec 1975, pp. 1502-1511.

[9]Fried, D. L., "Optical Heterodyne Detection of an Atmospherically Distorted Signal Wave Front", *Proceedings of the IEEE*, Vol. 55, Jan 1967, pp 57-67.

[10]Dekany, R., Troy, M., Brack, G., Bleau, C., DuVarney, R. Ealey, M., "1600 Actuator Tweeter Mirror Upgrade for the Palomar Adaptice Optics Ssytem (PALAO)", *Proc. SPIE*, Vol. 4007, July 2000, pp. 175-179.

[11]Greenwood, D. P., and Fried, D. L., "Power Spectra Requirements for Wave-Front-Compensative Systems," *J. Opt. Soc. Am.*, Vol. 66, March 1976, pp 193-206.

[12]Greenwood, D. P., "Bandwidth Specification for Adaptive Optics Systems", *J. Opt. Soc. Am.*, Vol. 67, March 1977, pp 390-393.

[14]Chouinard, M., Asghar, A., Kirk, J. F., Siegenthaler, J. P., Jumper, E. J., "An Experimental Verification of the Weakly-Compressible Model," 40th AIAA Aerospace Sciences Meeting and Exhibit, Reno NV, Jan 2002.

[15]Siegenthaler, J. P., Gordeyev, S., Jumper, E. J., "Optical Characterization of a Forced Compressible Shear-Layer," 34th AIAA Plasmadynamics and Lasers Conference, Orlando FL, Jun 2003

[16]Buckner, A., Gordeyev, S., Jumper, E.J., "Optical Aberrations Caused by Transonic Attached Boundary Layers: Underlying Flow Structure," 43rd AIAA Aerospace Sciences Meeting and Exhibit, Reno, NV, Jan 2005.

[17]Cress, J.A., Gordeyev, S., Jumper, E.J., Ng, T.T., Cain, A.B., "Similarities and Differences in Aero-Optical Structure over Cylindrical and Hemispherical Turrets with a Flat Window," 45th AIAA Aerospace Sciences Meeting and Exhibit, Reno NV, Jan 2007.

[18]Golbraikh, E., Kopeika, N.S., "Behavior of Structure Function of Refraction Coefficients in Different Turbulent Fields," Applied Optics, Vol. 43, No. 33, 2004, pp. 6151-6156.

[19]Stribling, B. E., Welsh, B. M., Roggemann, M. C., "Optical Propagation in Non-Kolmogorov Atmospheric Turbulence," *Atmospheric Propagation and Remote Sensing IV, SPIE Proc.*, Vol. 2471, 1995.

[20]Rao, C., Jiang, W., Ling, N., "Adaptive-Optics Compensation by Distributed Beacons for Non-Kolmogorov Turbulence," Applied Optics, Vol. 40, No. 21, 2001, pp. 3441-3449.

[21]Merrill, B.R., "Equivalence of Two Theories of beam Tilt," *J. Opt. Soc. Am. A*, Vol. 8, No. 8, Aug 1991, pp. 1316-1318.

[22]Siegenthaler, J. P., Gordeyev, S., Jumper, E. J., "Apertures, Sub-apertures, and Corrective Bandwidths," 2006 Annual Directed Energy Symposium (Directed Energy Professional Society), Albuquerque NM, Oct 2006.

[23]Siegenthaler, J. P., Jumper, E. J., "Aperture Effects in Aero-Optics and Beam Control," *J. of Directed Energy*, Vol. 2, No. 4, Fall 2007, pp 325-346.